Evidence from accreted seamounts for a depleted component in the early Galapagos plume

Buchs et al.

Content of this file:

1. Tectonostratigraphic constraints on accretion ages

The age of accretion of the OIC is constrained by tectonostratigraphic observations at a regional scale. The inner part of the OIC is tectonically juxtaposed in the NE to the Golfito Complex that includes Upper Cretaceous to Eocene sequences of the early south Central American arc (Buchs et al., 2010). The OIC is partly covered by Upper Paleocene, arc-derived sedimentary rocks in the Burica Peninsula (Buchs et al., 2009). These data define a Late Cretaceous-Late Paleocene accretion age for the inner OIC. In the SW, the outer OIC is bounded by the Middle Eocene to Miocene Osa Mélange, for which several origins have been proposed: (1) accretion of olistostromes composed of material reworked from the margin and deposited in the trench (Di Marco et al., 1995); (2) dismemberment and deformation of basal sequences of the OIC due to tectonic erosion (Meschede et al., 1999); and (3), accretion of the volcano-sedimentary cover of a seamount chain partly preserved in the OIC (Vannucchi et al., 2006). However, detailed (1:5'000 scale) mapping combined with geochemical analysis of igneous blocks and biostratigraphic dating of the mélange matrix and sedimentary cover of the igneous blocks support only (1) above (Buchs et al., 2009). The main unit of the Osa Mélange in contact with the OIC includes deformed olistostromes composed of a complex assemblage of Upper Cretaceous to Middle Eocene material reworked from the volcanic arc and the OIC, which deposited in the trench in the Late Eocene shortly before accretion. Therefore, preceding observations constrain the age(s) of accretion of the outer OIC to pre-Late Eocene.

2. Accuracy of the LA-ICPMS trace element analysis of lithium tetraborate glass beads

The accuracy of LA-ICPMS data for lithium tetraborate glass beads depends on the correctness of the 'gas blank assumption', instrument performance / tuning (e.g., detection

system linearity, counting-analog conversion coefficients, dead time), potential matrix effects and interferences and quality of certification of the external standard chemical composition. Gas blank was used to characterize the background noise. This approach can be questioned, because the lithium tetraborate used to dissolve sample powders is not necessary pure, and because of the presence of spectral interferences. We regularly analyze 100% lithium tetraborate glass beads prepared from *Lithium Tetraborate Spectromelt A 10* from Merck, Cat. Nr. 1.10783.5000, using lithium as an internal standard. Impurities found are Ba, Zn, Cr, V, Sc (0.4 – 4 μg/g), with the V and Sc values being related to the presence of spectral overalps ($B^{11}Ar^{40+}$ and $Li^{7}Ar^{38+}$, respectively). All REE, as well as U, Th and Pb are below 20 ng/g. Such results allow using the 'gas blank' intensity as a reasonable proxy for the background for all igneous samples except rare, depleted compositions of dunite or troctolite affinity (see also details in Buchs et al., 2010).

The role of instrument performance / tuning is usually tested by analyzing a secondary standard with an external certification. We also perform such tests on a regular basis. Results relevant to this study are listed in Table DR3, and show accuracy better than ±15% for all rare earth elements, Nb, Th, U and Pb. Therefore no important inaccuracy was encountered for the elements used in this study.

3. List of geochemical datasets showed in Figure 2

- Boninites from the Izu-Bonin volcanic arc (data retrieved on http://georoc.mpch-mainz.gwdg.de/georoc/, 2014)
- Mid-ocean ridge basalts (MORB, superfast segment of the East Pacific Rise, Pollock et al., 2009).
- Off-axis seamounts from the East Pacific Rise (Niu et al., 1999)
- Cocos and Carnegie ridges (Harpp et al., 2005)
- Genovesa Island from the Galapagos archipelago (Harpp et al., 2003)
- Gorgona komatiites (Kerr, 2005; Kamenetski, 2010)
- Depleted basalts from ODP Site 1001 in the Caribbean Large Igneous Province (Kerr et al., 2009)
- Autochtonous oceanic plateau basalts from south Central America (Nicoya and Azuero Marginal complexes, Hauff et al., 2000 and Buchs et al., 2010)
- Oceanic island basalts (OIB) accreted elsewhere in south Central America (Quepos and Azuero, Hauff et al., 2000 and Buchs et al., 2011)
- Primitive Mantle values are after McDonough and Sun (1995).

4. Isotope data: methods, data selection and age correction

Nd-Pb isotope data on a subset of 7 samples from the outer OIC were analyzed at the GEOMAR Helmholtz Center (Kiel, Germany) following the methods of Hoernle et al. (2015), with relevant standard measurements in Table DR4.

The data used for reference fields in Figure 3 include only samples with Pb and Nd isotope data:

- EPR MORB field is based on the Petrological Database (PetDB v.2.8.6, retrieved on http://www.earthchem.org/, 2015). All samples come from the superfast EPR (5 to 25° S) and have La/Sm < 1.4. This selection was made based on the assumption that these segments would be the most likely to be similar to depleted basalts of the Osa Igneous Complex.
- Gorgona komatiites are from GEOROC Gorgona precompiled file (retrieved on http://georoc.mpch-mainz.gwdg.de/, 2015).
- IODP Site 1001 field is based on Kerr et al. (2009).
- Central America Oceanic Plateau field includes basalts from the Nicoya Complex in Costa Rica (Hauff et al., 2000).
- Genovesa island field includes basalt samples from White et al. (1993).

We have carefully considered age-correcting isotope values for our comparison between above reference datasets and Group 3 basalts and decided not to display these data in Figure 3. This decision is motivated by three main reasons.

First, we corrected radiogenic ingrowth in the studied basalts and reference datasets mentioned above back to 62 Ma (age of formation of Group 3 basalts), but this had no notable effects on our main conclusions based on dissimilar isotopic compositions between Group 3 basalts and EPR MORB. The effect of this correction on Group 3 is given in Table 1 below and on Figure 3 by a vector representing the average correction for radiogenic ingrowth.

Second, age correcting reference datasets is hampered by missing trace elements (Nd, Sm, Pb, U, and Th) in samples including isotope data. To compensate this limitation, we estimated missing traces before age correcting using an approach similar to that of Arevalo and McDonough (2010) for the construction of "canonical" trace element ratios in a given tectonic setting. For example, missing trace elements in EPR MORB from the PETDB were

calculated using Pb = 0.1582 x La or 0.0536 x Nd, U = 0.0180 x La or 0.0158 x Nd, and Th = 0.0466 x La or 0.0061 x Nd, where the constants are based on global trace element values of N-MORB (Arevalo and McDonough, 2010). Missing trace elements in Gorgona komatiites and Genovesa island basalts were obtained using a similar approach, using average regional trace element ratios calculated based on GEOROC, respectively Harpp et al. (2003) data. Estimating missing trace element data offer a better assessment of the compositional variability in a large sample population; notably, this allowed increasing the number of plotted EPR MORB samples from 33 to 83. However, this approach also introduces scattering in the data (see Figure 1 below) and, therefore, is of relatively limited interest to compare our samples with reference datasets.

Finally, correction of radiogenic ingrowth should be focused on the composition of the source of the basalts, and not only the composition of the basalts at the time of eruption, because Th/Pb, U/Pb, and Sm/Nd ratios increase during partial melting and fractional crystallization; this can subsequently lead to significant, diverging isotopic evolution of the source residue and melting products. Therefore, to further compare the source of Group 3 basalts with that of modern EPR MORB, we modelled the radiogenic ingrowth of the source of Group 3 basalts from 62 Ma to present, assuming that trace elements in the source were similar to that of depleted DMM (values of Workman and Hart, 2005). Isotopic values of Group 3 basalts age-corrected back to 62 Ma were used as the starting composition of the source of these basalts. Our results indicate there is very little difference between isotopic compositions of Group 3 basalts and their source at present (Table 1 below). In other words, this two-step approach shows that the composition of Group 3 basalts in Figure 3 is virtually identical to that of their source at present, which clearly supports isotopic dissimilarity between the source of Group 3 basalts and that of EPR MORB. However, it is important to remember that the validity of this approach relies on the assumption that trace elements in the source residue of Group 3 basalts are similar to those of depleted DMM *sensu* Workman and Hart (2005).

In summary, age correction introduces both advantages and disadvantages, which in any case plays a very limited role in the comparison of relatively young depleted igneous rocks (i.e. Group 3 basalts and Gorgona Komatiites) and modern EPR MORB. Importantly, whichever technique was used we consistently observed a clear isotopic dissimilarity between EPR MORB and Group 3 basalts, with isotopic similarity between Group 3 basalts and Gorgona komatiites.

$^{206/204}$Pb	$^{208/204}$Pb	εNd	
-0.105	-0.054	-0.360	Correction for radiogenic ingrowth in the basalts
0.079	0.057	0.513	Radiogenic ingrowth of the source
-0.026	0.004	0.154	Combined effects (source at present)

Table 1. Average isotopic variations of Group 3 basalts and their source with age correction (62 Ma). See text for explanations.

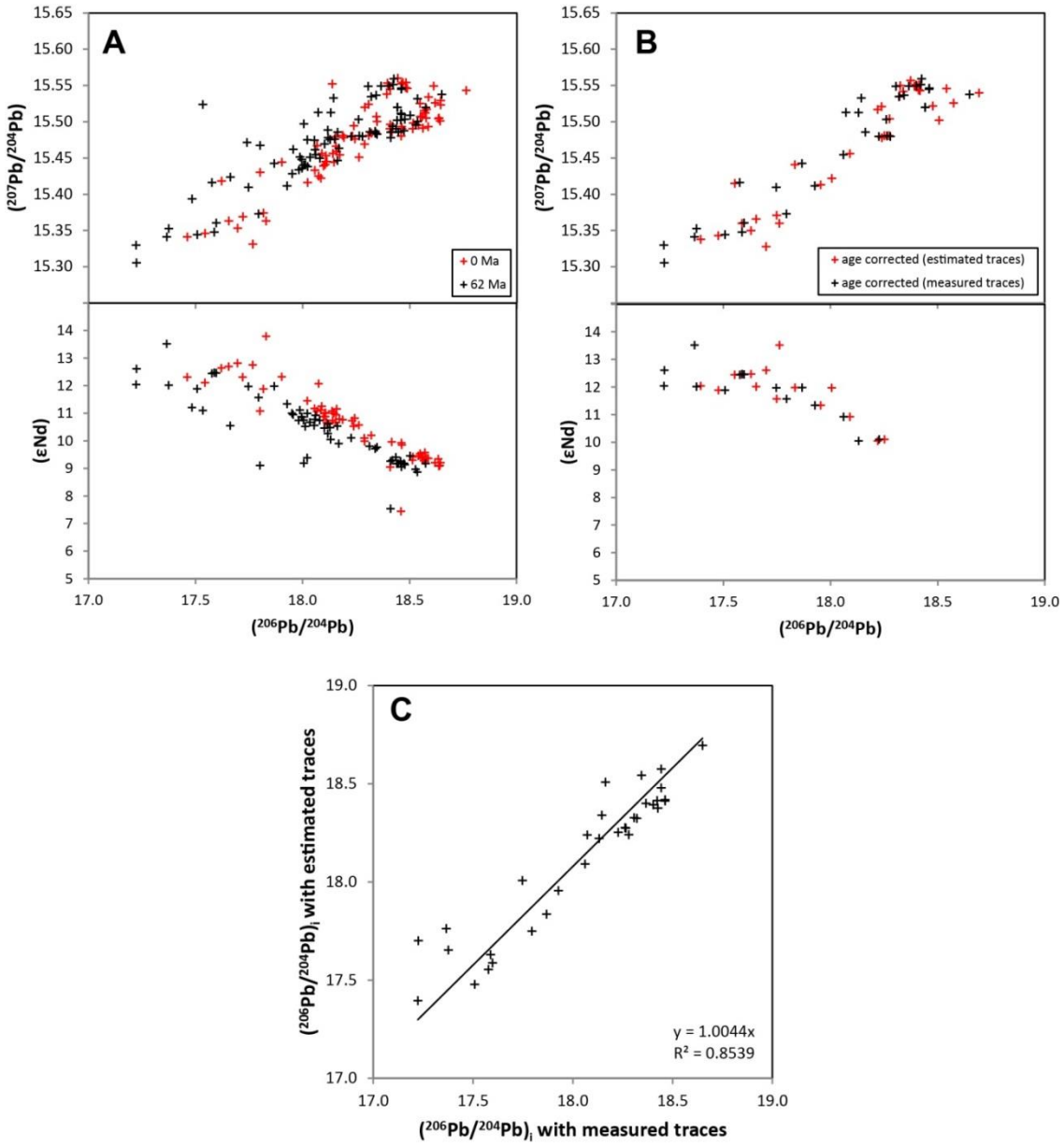

Figure 1. Effects of age correction on EPR MORB radiogenic isotope data (sources given above) using measured and estimated trace element ratios. (A) Full dataset with measured and estimated trace elements. Note increased data scattering for the initial ratios (in particular εNd_i). (B) Sample subset with complementary radiogenic isotope and trace element data. (C) Comparison of initial $^{206}Pb/^{204}Pb$ using measured and estimated U/Pb in the same sample subset as (B); note scattering of the data due to estimation technique.

References

Buchs, D. M., Arculus, R. J., Baumgartner, P. O., Baumgartner-Mora, C., and Ulianov, A., 2010, Late Cretaceous arc development on the SW margin of the Caribbean Plate: Insights from the Golfito, Costa Rica, and Azuero, Panama, complexes: Geochemistry Geophysics Geosystems, v. 11, no. 7, Q07S24.

Buchs, D. M., Arculus, R. J., Baumgartner, P. O., and Ulianov, A., 2011, Oceanic intraplate volcanoes exposed: Example from seamounts accreted in Panama: Geology, v. 39, no. 4, p. 335-338.

Di Marco, G., Baumgartner, P. O., and Channell, J. E. T., 1995, Late Cretaceous-early Tertiary paleomagnetic data and a revised tectonostratigraphic subdivision of Costa Rica and western Panama.; Geologic and tectonic development of the Caribbean Plate boundary in southern Central America, in Mann, P., ed., Geologic and Tectonic Development of the Caribbean plate boundary in southern Central America, Volume 295, p. 1-27.

Harpp, K. S., Fornari, D. J., Geist, D. J., and Kurz, M. D., 2003, Genovesa Submarine Ridge: A manifestation of plume-ridge interaction in the northern Galápagos Islands: Geochemistry Geophysics Geosystems, v. 4, no. 9, p. 8511.

Harpp, K. S., Wanless, V. D., Otto, R. H., Hoernle, K. A. J., and Werner, R., 2005, The Cocos and Carnegie Aseismic Ridges: a Trace Element Record of Long-term Plume-Spreading Center Interaction: Journal of Petrology, v. 46, no. 1, p. 109-133.

Hauff, F., Hoernle, K. A., van den Bogaard, P., Alvarado, G. E., and Garbe-Schonberg, D., 2000, Age and geochemistry of basaltic complexes in Western Costa Rica: Contributions to the geotectonic evolution of Central America: Geochemistry Geophysics Geosystems, v. 1, no. 5, p. 1009, doi:10.1029/1999GC000020.

Hoernle, K., Rohde, J., Hauff, F., Garbe-Schonberg, D., Homrighausen, S., Werner, R., and Morgan, J.P., 2015, How and when plume zonation appeared during the 132 Myr evolution of the Tristan Hotspot: Nature Communications, v. 6, p. 7799, doi:10.1038/ncomms8799.

Kamenetsky, V. S., Gurenko, A. A., and Kerr, A. C., 2010, Composition and temperature of komatiite melts from Gorgona Island, Colombia, constrained from olivine-hosted melt inclusions: Geology, v. 38, no. 11, p. 1003-1006.

Kerr, A. C., Pearson, D. G., and Nowell, G. M., 2009, Magma source evolution beneath the Caribbean oceanic plateau: new insights from elemental and Sr-Nd-Pb-Hf isotopic studies of ODP Leg 165 Site 1001 basalts, in James, K. H., Lorente, M. A., and Pindell,

J. L., eds., The Origin and Evolution of the Caribbean Plate, Volume 328, Geological Society, p. 809-827.

Kerr, A. C., 2005, La Isla de Gorgona, Colombia: A petrological enigma?: Lithos, v. 84, no. 1-2, p. 77-101.

McDonough, W. F., and Sun, S. S., 1995, The Composition of the Earth: Chemical Geology, v. 120, no. 3-4, p. 223-253.

Meschede, M., Zweigel, P., Frisch, W., and Voelker, D., 1999, Melange formation by subduction erosion: the case of the Osa melange in southern Costa Rica: Terra Nova, v. 11, no. 4, p. 141-148.

Niu, Y., Collerson, K. D., Batiza, R., Wendt, J. I., and Regelous, M., 1999, Origin of enriched-type mid-ocean ridge basalt at ridges far from mantle plumes: The East Pacific Rise at 11°20'N: Journal of Geophysical Research, v. 104, no. B4, p. 7067-7087.

Pollock, M. A., Klein, E. M., Karson, J. A., and Coleman, D. S., 2009, Compositions of dikes and lavas from the Pito Deep Rift: Implications for crustal accretion at superfast spreading centers: Journal of Geophysical Research, v. 114, no. B3, B03207.

Vannucchi, P., Fisher, D. M., Bier, S., and Gardner, T. W., 2006, From seamount accretion to tectonic erosion; formation of Osa melange and the effects of Cocos Ridge subduction in southern Costa Rica: Tectonics, v. 25, TC2004, doi:2010.1029/2005TC001855.

White, W. M., McBirney, A. R., and Duncan, R. A., 1993, Petrology and Geochemistry of the Galápagos Islands: Portrait of a Pathological Mantle Plume: Journal of Geophysical Research, v. 98, no. B11, p. 19533-19563.

Workman, R. K., and Hart, S. R., 2005, Major and trace element composition of the depleted MORB mantle (DMM): Earth and Planetary Science Letters, v. 231, no. 1-2, p. 53-72.

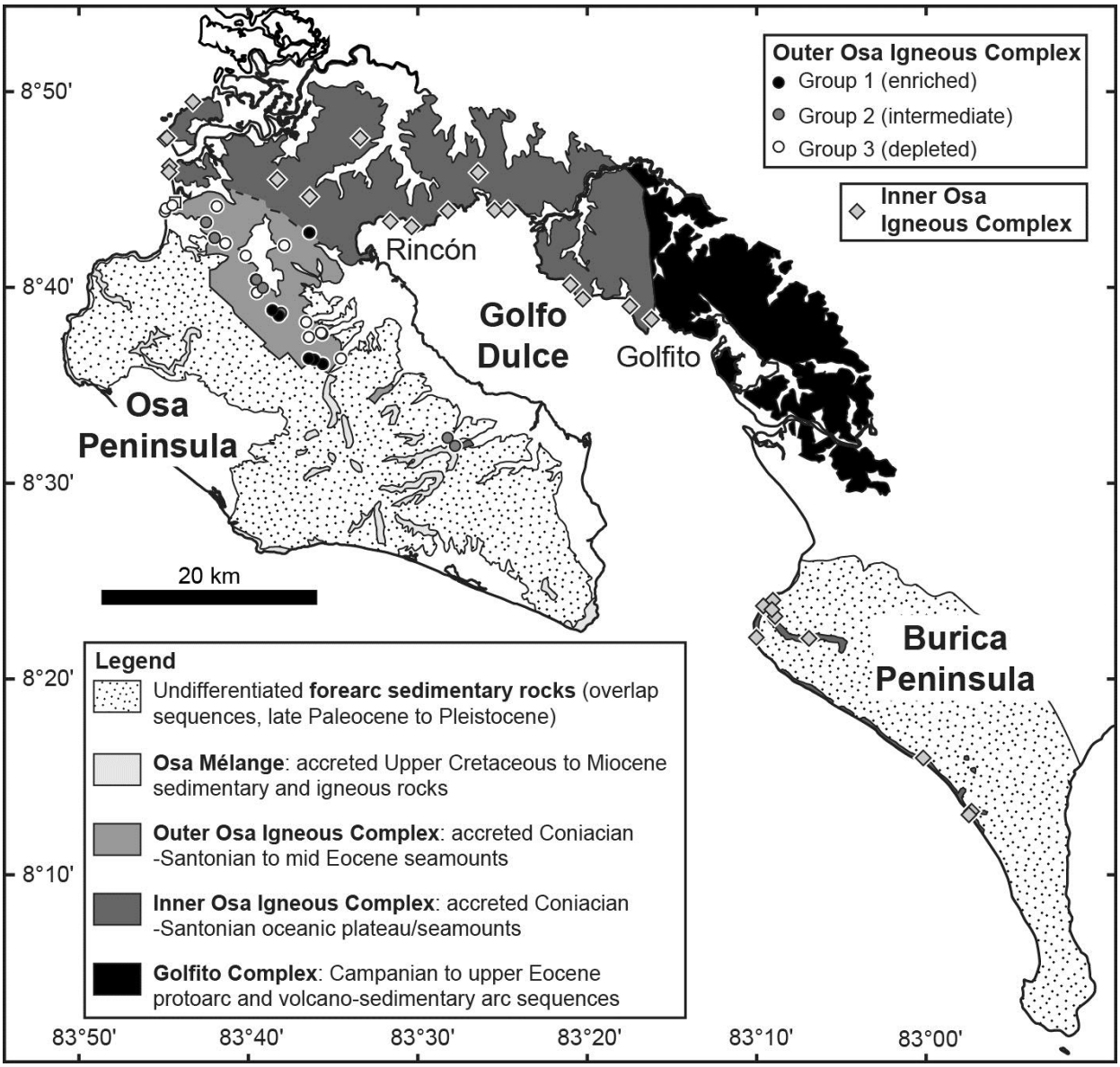

Figure DR1. General tectonic setting and simplified geological map of the studied area (modified after Buchs et al., 2009), also displaying the location of the samples used in this study (circle symbols for new geochemical analyses and squares symbols for data by Hauff et al., 2000).

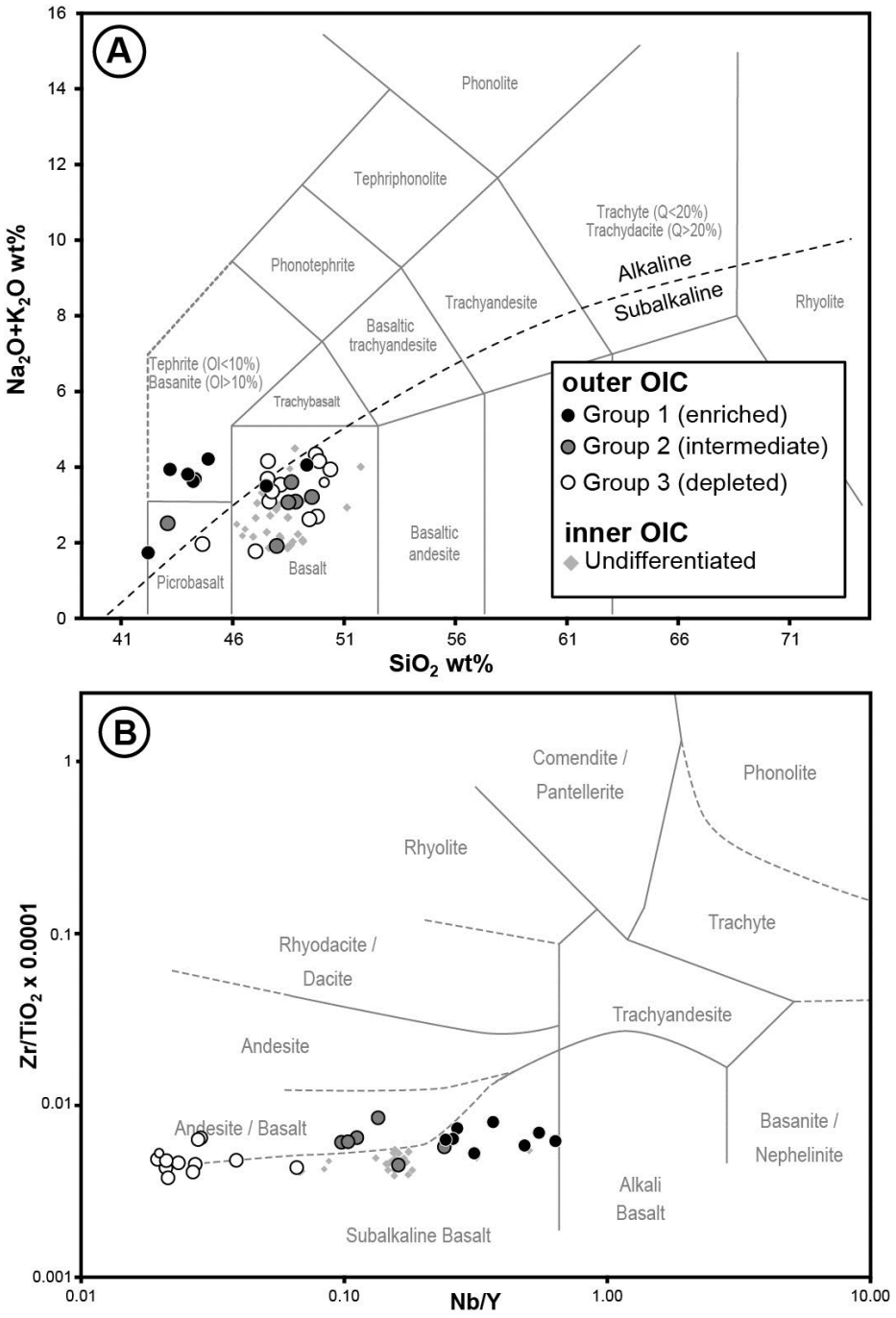

Figure DR2. TAS (A) and Winchester and Floyd (1977) (B) diagrams outlining compositional variation (essentially alkalinity) among the geochemical groups of the outer Osa Igneous Complex and basalts of the inner Osa Igneous Complex.

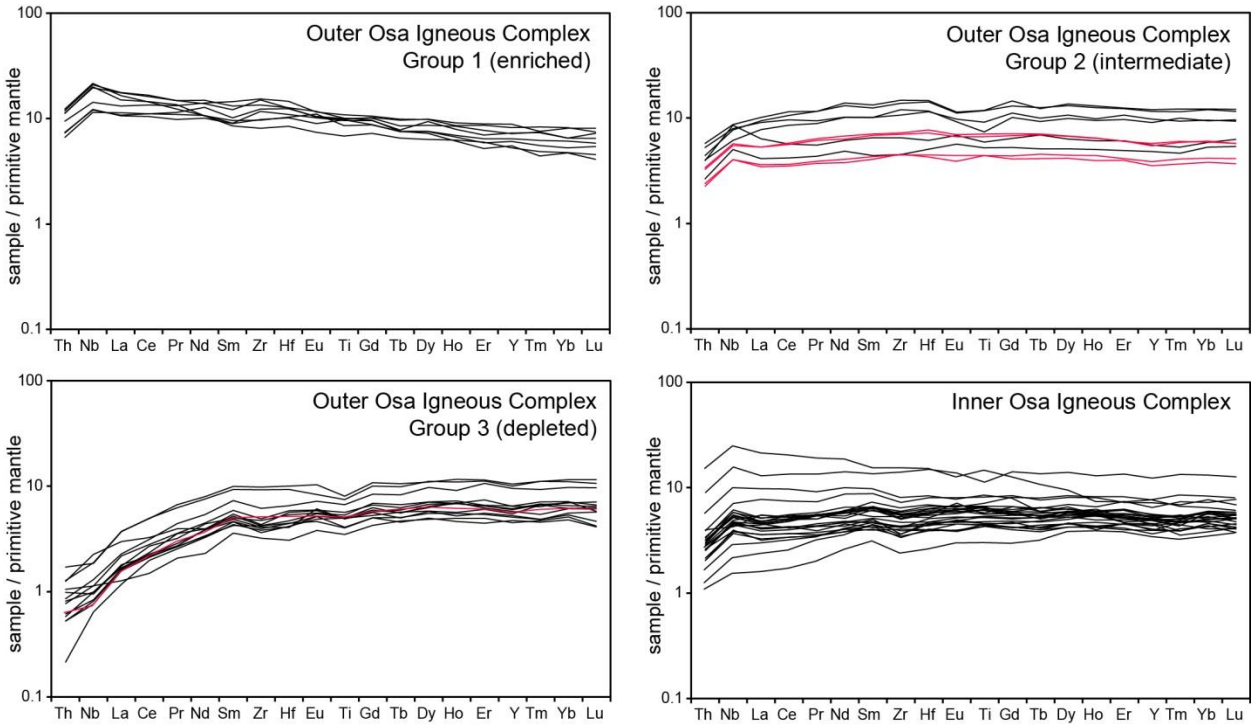

Figure DR3. Primitive mantle-normalized multielement diagrams used for the definition of geochemical groups in the outer Osa Igneous Complex. Samples in orange are from Hauff et al. (2000).

Table DR1. Location of analyzed samples

Sample	Unit	Rock type	Geochemical group	Northing	Easting
DB02-191	outer OIC	Basalt	Group 1	8.71289	-83.52766
DB02-242	outer OIC	Basalt	Group 1	8.64599	-83.55857
DB02-250	outer OIC	Basalt	Group 1	8.60529	-83.52406
DB05-113	outer OIC	Basalt	Group 1	8.60213	-83.51498
DB05-119	outer OIC	Basalt	Group 1	8.60665	-83.52678
DB05-121	outer OIC	Basalt	Group 1	8.60710	-83.52679
DB05-153	outer OIC	Basalt	Group 1	8.66724	-83.56493
DB05-161	outer OIC	Basalt	Group 1	8.64374	-83.55403
DB02-198b	outer OIC	Basalt	Group 2	8.72196	-83.61580
DB02-260	outer OIC	Basalt	Group 2	8.70839	-83.60854
DB02-261	outer OIC	Basaltic dyke	Group 2	8.70839	-83.60854
DB05-149	outer OIC	Dolerite	Group 2	8.66588	-83.56765
DB05-155	outer OIC	Basalt	Group 2	8.67313	-83.57356
DB05-156	outer OIC	Basalt	Group 2	8.67312	-83.57329
DB02-196	outer OIC	Basalt	Group 3	8.62699	-83.51678
DB02-197	outer OIC	Basalt	Group 3	8.62789	-83.51769
DB02-198a	outer OIC	Basalt	Group 3	8.62789	-83.51769
DB02-207	outer OIC	Basalt	Group 3	8.70205	-83.54947
DB02-216	outer OIC	Basalt	Group 3	8.73552	-83.60671
DB02-239	outer OIC	Basalt	Group 3	8.63694	-83.53041
DB05-114	outer OIC	Basalt	Group 3	8.60596	-83.50089
DB05-135	outer OIC	Basalt	Group 3	8.62383	-83.52814
DB05-152	outer OIC	Gabbro	Group 3	8.66182	-83.57265
DB05-158	outer OIC	Gabbro	Group 3	8.69347	-83.58218
DJ01-104	outer OIC	Basalt	Group 3	8.73100	-83.65125
DJ01-106	outer OIC	Basalt	Group 3	8.73371	-83.65034
DJ01-107	outer OIC	Basalt	Group 3	8.73643	-83.64488
DB02-107	inner OIC	Basalt	n/a	8.73269	-83.37315
DB02-110	inner OIC	Basalt	n/a	8.73268	-83.35588
DB02-119	inner OIC	Basalt	n/a	8.66753	-83.30414
DB02-120	inner OIC	Basalt	n/a	8.65667	-83.29416
DB02-132	inner OIC	Basalt	n/a	8.65030	-83.25419
DB02-135	inner OIC	Basalt	n/a	8.63943	-83.23603
DB02-160	inner OIC	Basalt	n/a	8.71828	-83.44041
DB02-165	inner OIC	Basalt	n/a	8.73181	-83.40950
DB02-201	inner OIC	Basalt	n/a	8.79607	-83.48672
DB02-203	inner OIC	Basalt	n/a	8.79425	-83.48490
DB02-204	inner OIC	Basalt	n/a	8.79425	-83.48490
DB02-230	inner OIC	Basalt	n/a	8.72280	-83.45858
DB02-246	inner OIC	Basalt	n/a	8.75902	-83.55490
DB02-266	inner OIC	Basalt	n/a	8.82413	-83.62761
DB05-107	inner OIC	Basalt	n/a	8.53108	-83.40329
DB05-108	inner OIC	Basalt	n/a	8.53832	-83.41009
DB06-054	inner OIC	Basalt	n/a	8.38612	-83.13055
DB06-058	inner OIC	Basalt	n/a	8.36709	-83.10153
DB06-061	inner OIC	Basalt	n/a	8.36816	-83.14595
DB06-065	inner OIC	Basalt	n/a	8.33269	-83.11187
DB06-066	inner OIC	Basalt	n/a	8.33191	-83.11064
DB06-070	inner OIC	Basalt	n/a	8.26539	-83.00409
DB06-075	inner OIC	Dolerite	n/a	8.33737	-83.11839
DJ01-022	inner OIC	Basalt	n/a	8.76537	-83.64761
DJ01-115	inner OIC	Basalt	n/a	8.79430	-83.64942
GDM-90303	inner OIC	Basalt	n/a	8.40063	-83.13264
GDM-91044	inner OIC	Basalt	n/a	8.39248	-83.13266

Table DR2. XRF analytical results (wt%)

Sample	Group	SiO_2	TiO_2	Al_2O_3	Fe_2O_3	MnO	MgO	CaO	Na_2O	K_2O	P_2O_5	LOI	Total
DB02-191	Group 1	47.51	1.96	13.50	12.27	0.18	7.06	9.65	3.31	0.19	0.16	3.42	99.22
DB02-242	Group 1	42.20	1.37	14.05	12.54	0.15	12.35	9.29	1.56	0.18	0.14	5.45	99.29
DB02-250	Group 1	44.23	2.02	16.46	12.99	0.17	7.85	7.31	2.90	0.74	0.20	4.36	99.23
DB05-113	Group 1	44.91	2.04	17.19	10.62	0.14	8.07	8.45	2.45	1.76	0.23	3.15	99.02
DB05-119	Group 1	43.19	2.18	15.77	13.99	0.22	8.40	6.89	3.32	0.63	0.23	4.30	99.12
DB05-121	Group 1	43.99	1.94	16.41	13.27	0.16	7.44	8.04	3.06	0.76	0.18	3.61	98.86
DB05-153	Group 1	49.34	1.97	14.70	9.62	0.16	7.03	9.65	3.66	0.40	0.25	2.66	99.43
DB05-161	Group 1	44.33	1.73	15.10	10.77	0.14	6.91	12.41	3.25	0.45	0.17	4.15	99.42
DB02-198b	Group 2	43.09	1.19	17.76	11.01	0.14	6.96	12.08	2.20	0.32	0.19	3.81	98.75
DB02-260	Group 2	49.56	1.49	15.47	11.05	0.18	6.31	9.96	3.09	0.13	0.15	1.69	99.07
DB02-261	Group 2	48.50	2.36	13.34	14.50	0.26	6.41	9.34	2.98	0.10	0.23	1.47	99.49
DB05-149	Group 2	47.98	1.05	13.91	11.96	0.18	9.08	11.28	1.78	0.14	0.08	2.08	99.53
DB05-155	Group 2	48.83	1.84	13.54	13.20	0.23	6.89	10.38	2.97	0.12	0.17	1.05	99.23
DB05-156	Group 2	48.64	2.40	13.17	15.20	0.26	6.03	8.80	3.44	0.17	0.22	1.13	99.44
DB02-196	Group 3	47.76	1.00	14.14	11.02	0.18	7.32	10.65	3.48	0.03	0.08	3.64	99.30
DB02-197	Group 3	47.65	1.07	15.79	11.61	0.20	6.71	11.11	2.81	0.28	0.08	1.97	99.27
DB02-198a	Group 3	48.15	1.02	15.28	11.44	0.20	7.75	9.55	3.10	0.44	0.07	2.41	99.41
DB02-207	Group 3	44.64	0.70	12.86	12.02	0.16	13.57	8.19	1.71	0.27	0.07	5.22	99.40
DB02-216	Group 3	47.03	0.82	16.86	9.83	0.18	6.90	13.66	1.75	0.03	0.06	2.22	99.33
DB02-239	Group 3	47.57	1.50	13.11	14.03	0.21	6.36	9.98	3.67	0.03	0.14	2.72	99.32
DB05-114	Group 3	49.45	1.35	13.09	15.01	0.22	6.40	10.68	2.58	0.05	0.09	0.55	99.46
DB05-135	Group 3	47.77	1.62	14.20	13.97	0.23	6.29	10.57	3.15	0.21	0.14	1.36	99.50
DB05-152	Group 3	47.59	0.81	20.44	7.69	0.13	5.45	10.79	2.25	1.91	0.06	2.09	99.21
DB05-158	Group 3	49.79	0.99	14.82	8.98	0.15	7.58	13.04	2.58	0.12	0.07	1.01	99.13
DJ01-104	Group 3	49.73	1.13	14.31	11.20	0.25	6.19	9.67	3.43	0.91	0.10	3.06	99.97
DJ01-106	Group 3	49.88	1.00	13.97	10.62	0.18	6.04	11.04	3.71	0.46	0.08	2.95	99.92
DJ01-107	Group 3	50.40	1.01	13.92	11.05	0.19	6.51	11.08	3.56	0.38	0.08	1.81	99.99
DB02-107	inner OIC	47.63	1.08	14.61	11.19	0.34	8.37	12.85	1.81	0.06	0.09	1.90	99.92
DB02-110	inner OIC	46.92	1.25	14.06	12.56	0.22	7.88	11.71	2.06	0.10	0.10	2.18	99.05
DB02-119	inner OIC	48.08	1.71	14.18	10.22	0.17	7.16	11.26	3.20	0.29	0.14	2.77	99.18
DB02-120	inner OIC	48.62	1.12	14.29	12.62	0.20	7.66	11.70	1.89	0.06	0.09	1.48	99.74
DB02-132	inner OIC	48.94	1.34	14.25	11.49	0.17	7.81	12.42	2.16	0.07	0.11	1.28	100.03
DB02-135	inner OIC	48.16	1.23	14.55	11.37	0.22	7.55	12.33	2.04	0.09	0.10	1.94	99.57
DB02-160	inner OIC	46.19	1.10	13.92	13.19	0.18	8.00	11.31	2.36	0.14	0.08	2.66	99.10
DB02-165	inner OIC	48.70	0.86	14.41	10.69	0.19	8.92	12.45	1.95	0.08	0.07	1.77	100.09
DB02-201	inner OIC	46.45	0.63	19.25	8.93	0.16	6.12	13.09	2.10	0.09	0.05	3.12	99.99
DB02-203	inner OIC	48.80	1.64	13.07	15.89	0.25	5.98	6.92	4.37	0.13	0.13	2.85	100.03
DB02-204	inner OIC	47.11	1.13	14.44	12.45	0.20	6.64	10.17	2.72	0.34	0.09	4.21	99.49
DB02-230	inner OIC	48.12	1.28	13.84	12.56	0.35	7.24	12.00	2.09	0.09	0.11	1.43	99.11
DB02-246	inner OIC	51.14	1.16	13.46	14.55	0.23	5.17	8.79	2.80	0.13	0.13	1.57	99.12
DB02-266	inner OIC	48.09	1.32	13.44	13.69	0.22	7.16	9.99	2.73	0.28	0.09	2.19	99.20
DB05-107	inner OIC	48.50	0.89	14.47	10.63	0.20	8.68	12.82	1.78	0.09	0.07	1.19	99.32
DB05-108	inner OIC	47.68	0.91	14.61	11.10	0.18	9.13	10.55	2.50	0.23	0.07	2.20	99.16
DB06-054	inner OIC	48.47	0.90	14.78	10.75	0.16	9.01	12.92	1.78	0.08	0.07	0.68	99.59
DB06-058	inner OIC	47.53	1.29	14.24	12.75	0.23	7.62	12.10	2.23	0.06	0.11	2.02	100.17
DB06-061	inner OIC	51.76	2.28	11.57	18.08	0.26	2.65	6.86	3.94	0.07	0.24	1.42	99.12
DB06-065	inner OIC	46.57	0.96	15.09	11.72	0.23	8.18	12.35	2.22	0.15	0.07	2.04	99.57
DB06-066	inner OIC	47.33	2.96	13.66	14.24	0.21	6.29	10.58	2.77	0.56	0.29	1.24	100.13
DB06-070	inner OIC	47.80	1.05	14.27	11.43	0.17	8.28	11.13	3.02	0.07	0.08	2.95	100.25
DB06-075	inner OIC	48.57	1.48	13.08	15.78	0.24	6.17	9.26	3.68	0.29	0.12	1.67	100.31
DJ01-022	inner OIC	47.04	0.88	14.73	10.66	0.16	8.33	12.41	2.54	0.12	0.07	2.95	99.89
DJ01-115	inner OIC	47.67	1.25	13.89	11.92	0.21	7.85	11.06	2.77	0.19	0.11	2.87	99.79
GDM-90303	inner OIC	49.13	0.96	14.13	11.18	0.18	8.13	11.16	2.29	0.81	0.08	1.88	99.93
GDM-91044	inner OIC	49.16	0.86	14.60	10.54	0.18	8.62	12.29	1.85	0.18	0.06	1.47	99.81

Table DR3. LA-ICP-MS analytical results (ppm)

Sample	Group	Sc	V	Ni	Rb	Sr	Y	Zr	Nb	Cs	Ba	La	Ce	Pr	Nd	Sm	Eu	Gd	Tb	Dy	Ho	Er	Tm	Yb	Lu	Hf	Pb	Th	U
DB02-191	Group 1	43.6	368	85	2.67	251	26	103	8.07	0.188	95.2	6.914	17.541	2.497	12.672	3.657	1.383	4.796	0.743	5.073	0.994	2.577	0.378	2.323	0.366	2.883	1.145	0.580	0.189
DB02-242	Group 1	40.2	276	bdl	3.72	154	23	85	14.21	0.315	48.5	10.717	24.136	3.143	13.318	3.462	1.144	3.948	0.647	4.280	0.933	2.620	0.330	2.094	0.307	2.398	1.450	0.980	0.268
DB02-250	Group 1	35.1	268	89	13.52	362	31	129	7.93	1.957	107.5	6.984	18.656	2.907	15.988	4.148	1.619	5.484	0.846	5.817	1.262	3.389	0.507	2.877	0.438	3.526	1.047	0.588	0.189
DB05-113	Group 1	32.0	278	147	18.86	606	24	142	12.91	bdl	362.1	11.375	27.169	3.764	18.722	5.342	1.801	5.263	0.749	4.873	0.911	2.277	0.301	2.084	0.277	3.609	0.836	0.898	0.271
DB05-119	Group 1	37.8	290	137	15.07	623	35	161	9.42	bdl	157.7	8.559	22.530	3.377	17.603	5.877	1.776	5.766	0.978	6.628	1.280	3.785	0.566	3.632	0.506	4.130	0.708	0.751	0.211
DB05-121	Group 1	37.2	277	92	16.45	437	31	123	7.54	bdl	116.7	7.389	18.610	2.776	13.446	3.662	1.574	5.205	0.773	6.347	1.183	3.072	0.502	2.890	0.491	3.108	0.886	0.529	0.271
DB05-153	Group 1	45.2	365	70	4.45	240	38	158	13.81	bdl	59.9	11.446	27.941	3.768	17.421	4.938	1.587	5.599	0.958	6.672	1.363	3.920	0.515	3.575	0.548	3.566	0.434	0.946	0.312
DB05-161	Group 1	46.7	339	122	12.59	203	28	102	13.25	bdl	65.4	9.728	24.386	3.462	13.335	3.887	1.697	4.753	0.750	5.126	1.032	2.834	0.421	2.696	0.395	2.927	0.423	0.890	0.842
DB02-198b	Group 2	39.0	249	bdl	5.72	244	24	69	5.66	0.131	144.0	4.144	9.549	1.418	7.727	2.654	1.064	3.506	0.689	4.281	0.914	2.687	0.362	2.595	0.427	1.746	3.145	0.314	0.000
DB02-260	Group 2	41.0	323	bdl	1.34	171	39	127	5.24	bdl	24.6	5.922	16.249	2.395	12.819	4.140	1.425	5.526	0.923	6.714	1.421	4.267	0.685	4.183	0.653	3.319	0.637	0.419	0.133
DB02-261	Group 2	48.7	460	49	1.44	144	50	146	5.11	0.031	20.5	6.146	17.779	2.962	16.533	5.086	1.732	7.143	1.249	8.883	1.878	5.386	0.787	5.311	0.785	4.059	28.839	0.353	0.132
DB05-149	Group 2	59.0	392	153	1.80	95	21	48	3.31	bdl	61.6	2.679	7.025	1.110	6.087	1.800	0.878	2.876	0.509	3.467	0.753	2.171	0.317	2.350	0.364	1.440	0.284	0.212	0.079
DB05-155	Group 2	49.2	412	65	1.19	150	42	113	4.06	bdl	31.8	5.042	14.397	2.265	12.773	4.140	1.515	6.104	0.997	7.251	1.470	4.687	0.636	4.245	0.635	3.258	0.710	0.319	0.090
DB05-156	Group 2	52.3	515	48	1.68	177	52	156	5.75	bdl	34.0	6.576	19.380	2.961	17.547	5.453	1.768	7.956	1.224	9.222	1.944	5.486	0.834	5.407	0.820	4.178	0.643	0.459	0.162
DB02-196	Group 3	46.8	350	78	0.66	29	26	45	0.55	0.050	4.6	1.069	3.932	0.899	4.921	2.203	0.902	3.403	0.551	4.359	1.017	2.848	0.462	2.877	0.435	1.598	1.656	0.049	0.079
DB02-197	Group 3	49.7	330	68	4.63	128	28	50	0.65	0.590	50.6	1.135	4.521	0.815	5.510	2.020	0.855	3.744	0.664	4.770	1.079	2.880	0.483	3.141	0.389	1.515	1.470	0.046	0.000
DB02-198a	Group 3	48.9	320	67	6.45	143	26	45	0.53	0.383	47.6	1.045	3.794	0.728	4.819	2.119	0.843	3.116	0.588	4.555	1.016	2.852	0.454	3.060	0.480	1.329	1.232	0.042	0.048
DB02-207	Group 3	44.4	228	bdl	6.86	69	19	34	0.75	0.207	10.5	0.821	2.513	0.531	2.883	1.461	0.586	2.319	0.463	3.290	0.740	2.179	0.322	2.253	0.283	0.873	0.844	0.061	0.049
DB02-216	Group 3	49.1	282	96	0.90	83	22	40	0.42	bdl	1.4	0.760	3.309	0.648	4.096	1.759	0.794	2.729	0.500	3.710	0.821	2.358	0.329	2.460	0.385	1.164	0.885	0.017	0.030
DB02-239	Group 3	51.6	392	bdl	0.53	29	43	97	1.22	bdl	6.2	2.393	8.362	1.588	9.472	3.791	1.286	5.471	0.983	7.474	1.631	4.916	0.759	4.883	0.719	2.642	0.808	0.136	0.088
DB05-114	Group 3	54.2	474	54	0.54	66	41	65	0.85	bdl	13.4	1.476	5.242	1.121	6.749	2.956	1.111	4.564	0.823	6.549	1.363	4.650	0.636	4.285	0.652	1.855	0.244	0.068	0.031
DB05-135	Group 3	55.7	435	50	2.89	130	45	103	1.24	bdl	25.6	2.412	8.304	1.702	9.981	4.045	1.596	5.864	1.049	7.373	1.738	5.019	0.756	5.082	0.778	2.846	0.248	0.101	0.062
DB05-152	Group 3	39.1	254	66	29.27	194	20	44	0.62	bdl	1180.8	1.163	3.627	0.676	4.232	1.712	0.715	2.729	0.451	3.366	0.690	1.959	0.309	2.114	0.278	1.261	0.505	0.078	0.039
DB05-158	Group 3	53.9	333	127	0.80	112	23	43	1.48	bdl	12.4	1.935	5.481	1.008	4.953	1.975	0.944	3.071	0.498	3.876	0.781	2.432	0.331	2.356	0.314	1.153	0.261	0.100	0.034
DJ01-104	Group 3	43.3	313	47	20.36	108	28	52	0.75	0.220	58.3	1.414	4.681	0.905	5.600	2.391	0.917	3.603	0.622	4.745	1.030	3.241	0.435	3.127	0.448	1.657	1.719	0.083	0.124
DJ01-106	Group 3	44.0	304	66	7.53	107	24	38	0.50	0.150	10.8	1.023	3.533	0.681	4.178	1.861	0.750	2.866	0.562	3.933	0.840	2.643	0.453	2.717	0.423	1.185	1.077	0.042	0.033
DJ01-107	Group 3	45.8	320	53	7.88	111	25	42	0.65	0.142	30.0	1.091	3.754	0.689	4.854	1.882	0.794	3.229	0.560	4.207	1.044	2.713	0.366	2.691	0.412	1.252	1.445	0.064	0.081
DB02-107	inner OIC	50.8	314	114	0.86	103	20	49	3.00	0.042	27.8	2.706	7.145	1.102	5.921	2.076	0.793	2.976	0.542	3.521	0.816	2.270	0.331	2.062	0.343	1.339	0.698	0.205	0.076
DB02-110	inner OIC	48.8	331	101	1.08	129	21	58	3.60	0.036	17.5	3.119	8.500	1.406	7.561	2.453	0.872	3.076	0.538	3.975	0.841	2.379	0.340	2.353	0.321	1.552	1.081	0.252	0.088
DB02-119	inner OIC	46.5	340	85	4.09	231	21	85	6.62	0.027	54.0	6.380	16.343	2.332	12.564	3.999	1.206	4.353	0.589	4.433	0.850	2.073	0.303	1.805	0.275	2.374	0.596	0.454	0.135
DB02-120	inner OIC	52.5	355	94	0.68	112	21	53	3.64	0.047	19.7	3.027	8.211	1.371	6.414	2.501	1.098	3.106	0.500	3.858	0.848	2.264	0.341	2.633	0.342	1.593	0.991	0.235	0.109
DB02-132	inner OIC	51.7	357	93	0.86	116	23	63	3.82	0.014	34.4	3.333	9.346	1.481	8.157	2.649	1.027	3.623	0.592	4.234	0.853	2.484	0.369	2.470	0.372	1.891	0.740	0.270	0.093
DB02-135	inner OIC	50.0	341	109	0.94	143	22	58	3.54	0.031	39.9	3.132	8.535	1.418	7.150	2.660	0.960	2.995	0.568	3.998	0.929	2.285	0.324	2.492	0.381	1.592	0.912	0.253	0.091
DB02-160	inner OIC	54.3	350	73	2.04	101	24	47	1.96	0.031	118.0	2.009	5.568	0.901	5.327	1.956	0.773	2.921	0.530	4.183	0.897	2.791	0.372	2.661	0.411	1.334	0.822	0.137	0.050
DB02-165	inner OIC	49.4	302	128	1.02	97	17	36	2.60	0.037	14.7	2.057	5.668	0.888	4.786	1.640	0.612	2.163	0.377	2.845	0.626	1.747	0.265	1.918	0.253	1.108	1.109	0.162	0.063
DB02-201	inner OIC	39.7	233	68	1.75	195	15	26	1.05	0.026	20.0	1.077	2.990	0.530	3.371	1.313	0.479	1.678	0.327	2.697	0.605	1.733	0.229	1.591	0.262	0.770	0.810	0.090	0.038
DB02-203	inner OIC	52.8	459	38	1.94	47	31	76	4.68	0.030	6.4	5.012	12.469	1.873	10.893	3.568	1.235	4.575	0.758	5.463	1.195	3.181	0.469	3.405	0.466	2.272	1.292	0.311	0.097
DB02-204	inner OIC	48.6	348	76	4.62	165	22	54	3.23	0.093	47.2	3.541	8.820	1.403	6.726	2.619	0.927	3.208	0.527	3.733	0.839	2.303	0.319	2.193	0.348	1.652	0.925	0.227	0.075
DB02-230	inner OIC	49.9	352	98	0.98	107	24	62	3.86	0.021	16.2	3.077	9.101	1.402	7.476	2.451	1.044	3.378	0.645	4.183	0.895	2.747	0.348	2.600	0.369	1.804	0.989	0.239	0.086
DB02-246	inner OIC	46.3	410	22	1.98	123	28	58	2.81	0.024	57.8	3.565	8.797	1.286	7.630	2.667	0.979	3.577	0.634	4.691	0.985	3.252	0.501	3.205	0.524	1.772	1.003	0.317	0.100
DB02-266	inner OIC	50.7	406	72	4.51	130	23	56	4.05	0.105	22.0	3.350	8.861	1.393	7.257	2.166	0.972	2.999	0.537	3.696	0.812	2.456	0.362	2.297	0.370	1.469	0.910	0.263	0.093
DB05-107	inner OIC	49.8	314	147	1.10	130	19	44	3.14	bdl	16.2	2.624	7.025	1.107	5.844	1.955	0.699	2.551	0.409	3.100	0.697	1.974	0.317	2.124	0.301	1.247	0.318	0.206	0.074
DB05-108	inner OIC	50.1	330	127	3.08	128	20	45	3.04	bdl	24.3	2.678	7.123	0.991	5.661	1.701	0.759	2.272	0.419	3.083	0.633	1.977	0.265	2.009	0.286	1.237	0.218	0.201	0.052
DB06-054	inner OIC	49.5	305	128	1.40	135	16	35	2.41	bdl	23.2	2.117	5.695	0.884	5.102	1.733	0.601	2.310	0.396	2.843	0.641	1.815	0.277	1.876	0.307	1.146	0.485	0.162	0.087
DB06-058	inner OIC	51.3	357	107	0.64	202	24	59	3.44	bdl	115.3	2.950	8.368	1.282	7.418	2.691	0.947	3.228	0.637	4.233	0.887	2.673	0.361	2.647	0.396	1.711	0.575	0.250	0.089
DB06-061	inner OIC	44.6	321	8	0.85	53	53	148	10.39	bdl	18.5	8.413	22.512	3.422	17.806	5.509	2.126	7.703	1.348	9.419	1.943	5.911	0.908	5.819	0.858	4.223	0.504	0.716	0.220
DB06-065	inner OIC	52.3	311	106	1.41	123	22	39	1.47	bdl	741.9	1.602	4.446	0.845	4.639	1.883	0.774	2.569	0.498	3.655	0.827	2.332	0.305	2.596	0.357	1.313	0.307	0.104	0.038
DB06-066	inner OIC	38.7	399	87	6.50	291	33	163	16.53	bdl	384.3	13.900	34.374	4.891	23.416	6.297	1.952	6.892	1.067	6.404	1.108	3.233	0.456	2.862	0.413	4.328	0.817	1.219	0.397
DB06-070	inner OIC	52.8	356	108	0.92	230	21	44	3.12	bdl	31.3	2.933	6.944	1.157	6.003	1.873	0.812	2.750	0.518	3.561	0.736	2.158	0.317	2.235	0.342	1.445	0.350	0.204	0.077
DB06-075	inner OIC	50.1	414	43	4.48	141	34	70	2.96	bdl	69.3	2.968	8.249	1.418	7.737	3.070	1.045	4.574	0.822	5.866	1.274	3.737	0.604	3.820	0.564	2.023	0.338	0.224	0.081
DJ01-022	inner OIC	49.3	311	136	2.10	140	17	41	2.56	0.072	32.5	2.313	6.165	0.908	4.786	1.808	0.698	2.274	0.438	3.051	0.646	1.982	0.264	2.020	0.274	1.123	2.200	0.209	0.059
DJ01-115	inner OIC	48.2	330	103	2.58	157	22	58	3.42	0.095	116.5	2.929	8.279	1.383	7.163	2.576	0.902	3.211	0.584	3.873	0.825	2.361	0.376	2.217	0.349	1.651	2.793	0.253	0.117
GDM-90303	inner OIC	52.0	338	114	15.01	152	17	38	2.93	0.334	208.6	2.516	6.687	1.091	5.421	2.038	0.724	2.636	0.470	3.376	0.814	2.037	0.320	2.217	0.353	1.335	1.776	0.222	0.079
GDM-91044	inner OIC	48.2	304	132	3.04	250	19	43	2.51	0.213	79.6	2.326	6.096	0.956	5.010	1.612	0.593	2.308	0.395	3.115	0.593	2.010	0.240	1.678	0.281	1.131	2.075	0.170	0.091

bdl=beyond detection limit

Standard	Sc	V	Ni	Rb	Sr	Y	Zr	Nb	Cs	Ba	La	Ce	Pr	Nd	Sm	Eu	Gd	Tb	Dy	Ho	Er	Tm	Yb	Lu	Hf	Pb	Th	U
USGS GSP-2 (n=3)*	7.6	59	15	210	218	24	526	24	0.993	1241	171.019	408.097	49.407	189.554	24.253	2.085	11.978	1.158	5.343	0.831	2.142	0.283	1.512	0.228	12.919	38.168	99.756	2.268
Certified average	6.3	52	17	245	240	28	550	27		1340	180	410		200	27	2.3							1.6			42	105	2.4

**USGS GSP-2 granodiorite powder smelted with lithium tetraborate, Ca int.std., Pearce et al. 1997 + GeoRem SRM 612*

Table DR4. Radiogenic isotope data

Sample	Group	Age[(a)] (Ma)	Sm (ppm)	Nd (ppm)	$^{147}Sm/^{144}Nd$	$^{143}Nd/^{144}Nd_m$	$^{143}Nd/^{144}Nd_t$	εNd_t	Pb[(b)] (ppm)	U[(c)] (ppm)	Th (ppm)	$^{206}Pb/^{204}Pb_m$	$^{207}Pb/^{204}Pb_m$	$^{208}Pb/^{204}Pb_m$	$^{206}Pb/^{204}Pb_t$	$^{207}Pb/^{204}Pb_t$	$^{208}Pb/^{204}Pb_t$
DB05-113	Group 1	62	5.342	18.722	0.172	0.513063	0.512993	8.483	0.749	0.271	0.898	19.186	15.569	38.641	18.961	15.558	38.396
DB05-153	Group 1	62	4.938	17.421	0.171	0.512983	0.512914	6.935	0.697	0.312	0.946	19.373	15.588	38.823	19.094	15.575	38.544
DB05-155	Group 2	62	4.140	12.773	0.195	0.513094	0.513015	8.911	0.511	0.090	0.319	18.449	15.523	38.116	18.341	15.518	37.990
DB05-155 (replicate)	Group 2	62	4.140	12.773	0.195	0.513097	0.513018	8.960	0.511	0.090	0.319	18.457	15.524	38.125	18.349	15.519	38.000
DB02-197	Group 3	62	2.020	5.510	0.221	0.513221	0.513132	11.192	0.220	0.041	0.046	18.514	15.528	38.058	18.401	15.522	38.017
DB02-239	Group 3	62	3.791	9.472	0.241	0.513190	0.513093	10.424	0.379	0.088	0.136	18.686	15.527	38.092	18.544	15.521	38.020
DB05-114	Group 3	62	2.956	6.749	0.264	0.513227	0.513120	10.964	0.270	0.031	0.068	18.506	15.508	37.946	18.437	15.504	37.895
DB05-135	Group 3	62	4.045	9.981	0.244	0.513183	0.513084	10.251	0.399	0.062	0.101	18.700	15.525	38.136	18.605	15.520	38.085

(a) value used for the age correction, see Supplementary File 1 for a discussion on correcting radiogenic ingrowth

(b) based on Nd/Pb = 25±5.

(c) sample DB02-197 estimated.

Nd and Pb isotope ratios by TIMS in static multi collection mode on a TRITON Plus and MAT262 respectively. Mass bias correction uses $^{146}Nd/^{144}Nd = 0.7219$ and a ^{207}Pb-^{204}Pb double spike. Sample data are reported relative to $^{143}Nd/^{144}Nd = 0.511850 \pm 6$ (2SD, n = 114) for La Jolla and $^{206}Pb/^{204}Pb = 16.9427 \pm 21$, $^{207}Pb/^{204}Pb = 15.5005 \pm 21$, $^{208}Pb/^{204}Pb = 36.7278 \pm 46$, $^{208}Pb/^{206}Pb = 2.167765 \pm 63$ and $^{207}Pb/^{206}Pb = 0.914877 \pm 32$ (2SD, n = 17) for NBS981.

2016125_BuchsEtAl_Osa Igneous Complex_Tables.xlsx

- Table 1. Location of analyzed samples
- Table 2. XRF analytical results (wt%)
- Table 3. LA-ICP-MS analytical results (ppm)
- Table 4. Radiogenic isotope data